



www.sphinxsai.com

ChemTech

International Journal of ChemTech Research

CODEN (USA): IJCRGG ISSN: 0974-4290

Vol.8, No.5, pp 117-125, 2015

National conference on Nanomaterials for Environmental [NCNER-2015]

19th & 20th of March 2015

Removal of lead ions from aqueous solution by novel hydroxyapatite/alginate/gelatin composites

K. Sangeetha^{1*}, G. Vasugi¹, E. K. Girija¹

¹Department of Physics, Periyar University, Salem 636 011, India

Abstract: Accumulation of heavy metals in the aquatic environment from the industrial effluents is a major concern due to their toxicity and other adverse side effects. There is a high demand for economic and efficient adsorbents. In the present work, Pb²⁺ sorption capacity of hydroxyapatite-polymer (alginate and gelatin) composite adsorbents formed by simple wet precipitation method is studied. Sorption experiments are carried out by batch equilibrium method for different adsorbent dosages and reaction time. Complete removal was achieved within 24 hrs by both the adsorbents for both the dosages. Among the dosages studied (0.1 & 0.2 g) lower dose was found to exhibit maximum sorption capacity while the rate of removal was high for the higher dose. Presence of gelatin along with hydroxyapatite/alginate enhanced the sorption capacity of Pb²⁺.

Keywords : Adsorption; Heavy metal; Hydroxyapatite; Polymers; Composites.

1. Introduction

Most heavy metals are extremely toxic and non-biodegradable and their accumulation in soils, surface and ground waters due to various industrial and other effluent sources post a serious public health threat worldwide. Lead is a naturally occurring powerful neurotoxin heavy metal often released during metal smelting, mining and is a key component in car batteries^{1,2}. The health effects of lead exposure include neurological damage, reduced IQ, anemia, nerve disorders, lead colic and a number of other health problems such as convulsions, coma, delirium and possibly death^{3,4}. For the elimination of Pb, particularly in the form of free Pb²⁺ from the contaminated aqueous solutions, adsorption has received much attention due to its high efficiency and cost effectiveness^{5,6}. Other methods such as ion exchange, chemical precipitation, electrochemical reduction and electrodialysis are in use⁷⁻⁹. For physical adsorption, activated carbon is traditionally used as the adsorbent for the removal of Pb²⁺ owing to its high adsorption capacity, high porosity and very high surface area¹⁰. However, activated carbon is unable to selectively adsorb Pb²⁺, resulting in an unpredictable lifespan of the adsorbent¹¹.

Nowadays, technology is devoted to the development of novel nontoxic adsorbents which are capable of satisfying special requirements in terms of immobilization of heavy metal ions from aqueous media. Nanostructured materials exhibit steric effects on adsorption due to its very large surface area and it has abundant acceptor sites for adsorbates¹². Materials with functional groups such as phosphate, carboxyl, amide and/or amine exhibit significant heavy metal ion adsorption. Hydroxyapatite [HA, Ca₁₀(PO₄)₆(OH)₂] is one of the calcium phosphate phases with Ca/P ratio 1.67 and is the major component of natural bone and teeth¹³. Furthermore nano sized hydroxyapatite have been considered as an ideal low cost adsorbent due to their least solubility and high sorption capacity for metal ions^{14,15}. Alginate and gelatin are natural biopolymers which are

nontoxic, efficient, inexpensive and degradable. By introducing polymers rich in functional groups like amide and/or amine with HA, it is possible to derive large number of efficient composites for binding heavy metal ions¹⁶.

The aim of this work is to study the heavy metal sorption capacity of nanocomposites such as hydroxyapatite/alginate and hydroxyapatite/alginate/gelatin as a function of contact time and adsorbent dosage under batch equilibrium method.

2. Experimental

2.1. Materials and methods

Calcium nitrate tetrahydrate [Ca(NO₃)₂.4H₂O, 98%], di ammonium hydrogen phosphate [(NH₄)₂HPO₄, 99%], gelatin and ammonia solution [NH₄OH, 25%] were obtained from Merck. Sodium alginate and lead nitrate [Pb(NO₃)₂] were obtained from Loba chemie (India) and Himedia (India) respectively, all the reagents were used without further purification. Deionized water was employed as the solvent.

The calcium and phosphate solutions were prepared by dissolving 0.5 M calcium nitrate tetrahydrate and 0.3 M di ammonium hydrogen phosphate in water. pH of these solutions was brought above 10 using ammonia solution. The phosphate solution containing 6% of sodium alginate was added dropwise into the calcium solution under vigorous stirring at room temperature. The obtained suspension was stirred further for 1 hr and aged for 24 hrs. Then the resulting colloidal mixture was centrifuged to separate the product, washed thoroughly and dried at room temperature. The product obtained was named as HA/Alg (Hydroxyapatite/Alginate). The second adsorbent was prepared by mixing 1% gelatin to the calcium solution (0.5M) in the above experiment and this product was referred as HA/Alg/Gel(Hydroxyapatite/Alginate/Gelatin).

2.2. Sorption experiment

Pb²⁺ sorption experiment was performed by batch equilibrium method and the experiment was carried out for two adsorbent dosages (0.2 and 0.1g) in aqueous solution at 37°C. The adsorbent was added to 50ml of 2mM Pb(NO₃)₂ solution of pH 5 and aliquots were collected for predetermined time intervals 1, 4, 7, 24 and 29 hrs. Then the experiment was terminated and the adsorbent was filtered off, washed with deionized water and dried at room temperature for further analysis.

The amount of Pb²⁺ removed by unit mass of adsorbents at a given time is calculated by mass balance equation

$$q = \frac{v}{m} (c_0 - c) \text{ mM/g} \quad \dots \quad (1)$$

The removal efficiency of the adsorbents is calculated by the following equation

$$\text{Removal efficiency (\%)} = \frac{c_0 - c}{c_0} \times 100 \quad \dots \quad (2)$$

where v is the volume of the solution in litres, m is the mass of the adsorbent in grams, c₀ is the initial lead concentration in the solution in millimols per litre and c is the final concentration of lead ions after the time interval in millimols per litre.

2.3. Characterization

The phase composition and crystallographic structure of the adsorbents before and after sorption were identified by X-ray diffraction (PANalytical X' Pert PRO diffractometer) using CuK α radiation (1.5406 Å) with voltage and current setting of 40 kV and 30 mA respectively. The lattice parameters were calculated by the method of least square. The morphology of the adsorbents before and after sorption was examined in a high resolution scanning electron microscopy (FEI Quanta FEG 200- HR-SEM). ICP-OES (Perkin Elmer Optima 5300 DV) was used to determine the Ca and Pb²⁺ concentrations.

2.4. Kinetic models

The sorption kinetics of Pb²⁺ was analyzed on the basis of the two widely used kinetic models such as pseudo first and second order kinetic models.

The first order Lagergren equation pertaining to the adsorption rate is based on the adsorption capacity. It can be expressed as

$$\log(q_e - q_t) = \log q_e - \frac{k_1}{2.303} t \quad \dots \quad (3)$$

where q_t is the Pb^{2+} adsorbed at time t in millimol per gram, q_e is the amount of Pb^{2+} adsorbed at equilibrium in millimol per gram and k_1 is the adsorption rate constant. The slope of the straight line plots of $\log(q_e - q_t)$ against t will give the value of q_e , rate constant and regression coefficient.

2.4.2. The pseudo-second order kinetic model

The linearized second order kinetic model can be expressed as

$$\frac{t}{q_t} = \frac{1}{k_2 q_e^2} + \frac{1}{q_e} t \quad \dots \quad (4)$$

where q_t and q_e are the Pb^{2+} adsorbed on the surface of the adsorbents at time t and at equilibrium in millimols per gram respectively and k_2 is the rate constant. The slope of the straight line plots of t/q_t against t will give the value of q_e and rate constant.

2.5. Sorption isotherm

Adsorption isotherm studies are essential for elucidating the adsorption process at equilibrium conditions. An adsorption isotherm is characterized by certain constants which express the affinity of the adsorbent and can also be used to find the adsorption capacity of the sorbent. Two most widely used mathematical models Langmuir and Freundlich adsorption isotherms were adopted for expressing the quantitative relationship between the extent of sorption and the residual solute concentration.

Langmuir adsorption isotherm assumes the monolayer adsorption process on a homogeneous surface and the equation is expressed as¹⁷

$$q = \frac{q_{\max} bc}{1 + bc} \quad \dots \quad (5)$$

where q and q_{\max} represents the observed and maximum sorption capacities in millimol per gram. c is the concentration of metal ions in millimol per litre of solution, b is the equilibrium constant.

The Freundlich equation is an empirical expression that encompasses the heterogeneity of the adsorbent surface and the exponential distribution of sites and their energies. It can be expressed as

$$q = kc^n \quad \dots \quad (6)$$

where k is a constant representing sorption capacity and n is a constant representing adsorption intensity parameter.

2.6. Analysis of the variance (ANOVA)

The adequacy of the fit was determined by performing the analysis of variance on both the isotherm models. The sum of squares errors (SSE), the mean square error (MSE), F-ratio and prob>F were computed for each model.

$$SSE = \sum_{i=1}^m (q_{c,i} - q_i)^2 \quad \dots \quad (7)$$

$$MSE = \frac{SSE}{\text{Degree of freedom}} \quad \dots \quad (8)$$

where q_i and q_c are the experimental and calculated values of lead adsorbed onto the adsorbents, m is the number of experimental points. The mean square error (variance of the random error) can be measured by the ratio of sum of squared errors to the degree of freedom. F-ratios can be defined as the ratio of the respective mean square effect to the mean square error. The minimized error values, smaller values of prob>F and larger F-value indicate the significance of the model i.e, good fit with the experimental data.

3. Results and discussion

3.1. XRD

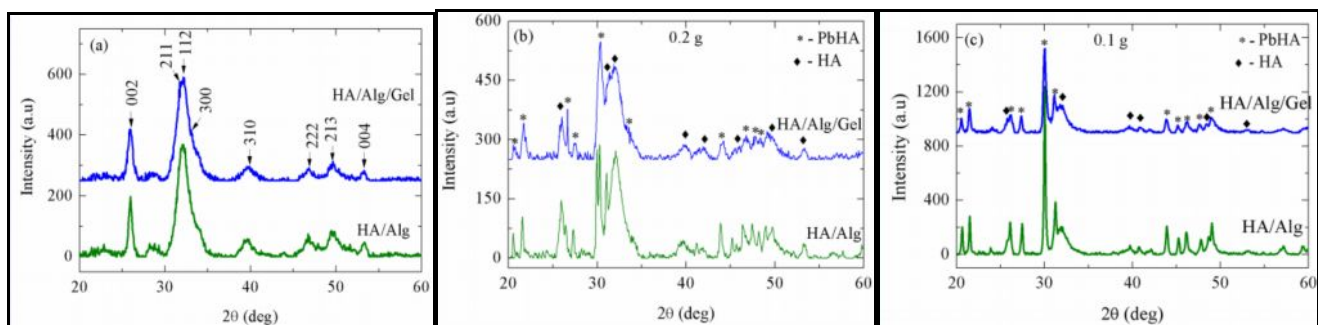


Fig. 1. XRD pattern of the adsorbents:(a) before sorption, (b) & (c) after sorption

Fig.1 are the XRD patterns of the adsorbents before and after the sorption experiment. From Fig.1(a), it was confirmed that the only mineral phase present in adsorbents was HA (JCPDS card no. 09-0432). Fig. 1.b and c shows the XRD patterns for the adsorbent dosages 0.2 and 0.1 g respectively after sorption experiment, which revealed the existence of two distinct phases, the parent HA phase and a new phase hydroxypyromorphite ($\text{Pb}_5(\text{PO}_4)_3\text{OH}$; card no.24-0586). The high crystalline nature of the newly formed hydroxypyromorphite phase is explicit from the sharp diffraction lines and is found to be the dominant phase in the lower dosage (0.1g). The lattice parameters a and c for hydroxyapatite obtained from the XRD pattern for the adsorbents before and after sorption of Pb^{2+} are given in Table 1.

Table1. Lattice parameters of the adsorbents before and after sorption

Adsorbents	Lattice parameters (\AA)					
	Before reaction		After reaction			
			0.2g dosage		0.1g dosage	
	a	c	a	c	a	c
HA/Alg	9.426	6.856	9.518	6.862	-	-
HA/Alg/Gel	9.383	6.878	9.675	6.902	-	-

After the Pb^{2+} sorption, both a and c of the parental HA increased in the case of 0.2g dosage. This may be due to the substitution of Pb^{2+} with large ionic radii (1.19 \AA) in the Ca^{2+} site (0.99 \AA). Whereas in lower dosage, most of the parent HA is converted into hydroxypyromorphite phase and no isolated peak of HA could be found to calculate the lattice parameters.

3.2. SEM

The microstructure of the HA/Alg composite before sorption experiment is shown in Fig 2A. HA spherulites uniformly embedded in the alginate matrix forming a compact block are observed. Whereas the mineral phase could not be distinguished even at higher magnification in the composite which contains gelatin along with alginate (Fig 2B). Influence of gelatin on the microstructure of Alg/HA composite has been reported by us recently¹⁸. After lead sorption, distinct large rod shaped crystals are observed for both the dosages. The size of the rods is about or less than 1 μm in the case of 0.2 g dosage (A1 & B1). The rods are found to originate from a central point forming flower shaped clusters in the HA/Alg/Gel adsorbent (B1).

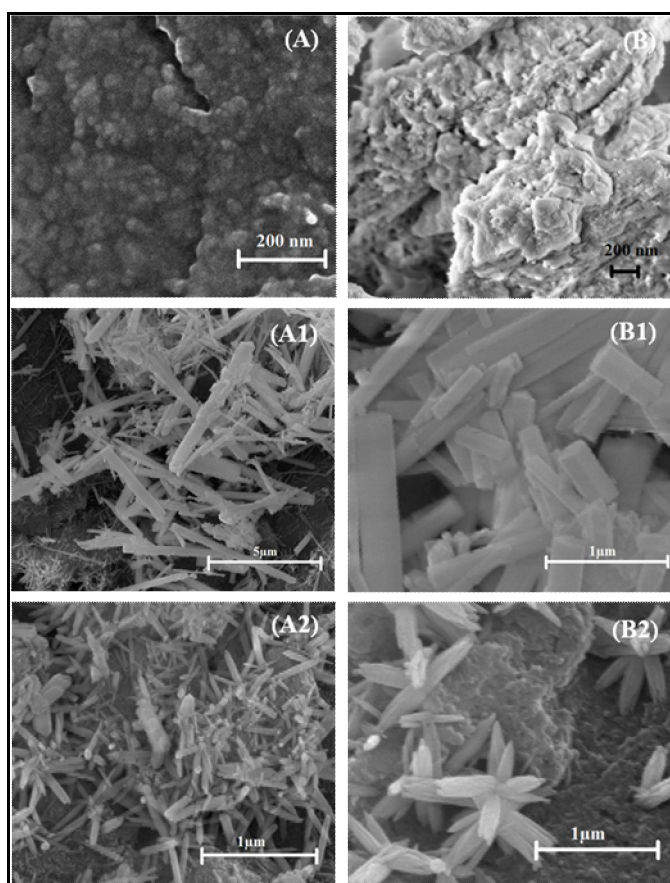


Fig. 2. SEM images of adsorbents before (A & B) and after (A1, B1- 0.2g ; A2, B2-0.1g) sorption

Large rods of 1 to 5 μm size are observed in the lower dosage of the adsorbent (A2 & B2). The morphology of the adsorbents changed completely after sorption and the rods observed may be the hydroxypyromorphite as it is confirmed from XRD.

3.3. Kinetic analysis

The sorption of Pb^{2+} on composite adsorbents is studied at different time intervals. The amount of Pb^{2+} removed (q) and removal efficiency(%) of both the adsorbents for dosages 0.2 and 0.1g deduced using equation (i) and (ii) at different time intervals are depicted in Fig.3 and Fig.4. The adsorption efficiency exhibited by HA/Alg/Gel was high in the first hour than by HA/Alg in both the dosages, after that the efficiency of the latter was found to be high. In higher dosage the efficiency of both the adsorbents are maximum at fourth and seventh hour than in the lower dosage and complete removal was achieved in 24 hrs by both the adsorbents for both the dosages. Comparison of two adsorbent dosages showed that fast removal was achieved in the case of higher dosage but the amount of Pb^{2+} removed by adsorbents was high for the lower dosage which is double the amount of Pb^{2+} removed by higher dosage.

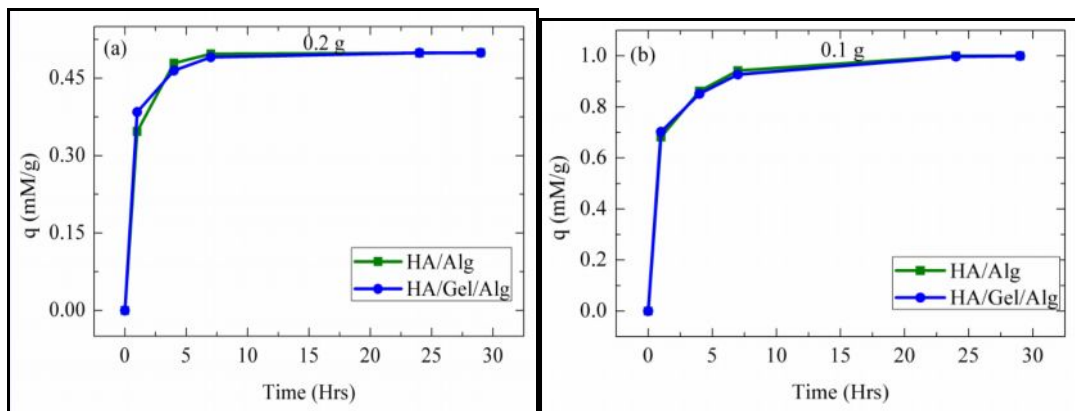
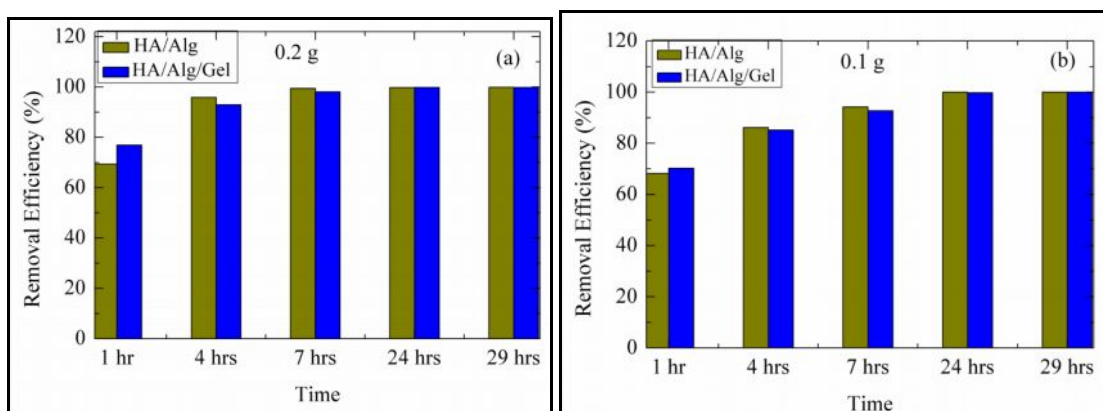


Fig. 3. Removal capacity of Pb^{2+} by the adsorbents

**Fig. 4. Removal efficiency of Pb^{2+} by the adsorbents**

The rate constants k_1 and k_2 , Pb^{2+} adsorbed at equilibrium (q_e) and regression coefficient (R^2) obtained from the plots of pseudo-first and second order rate equation for 0.2 and 0.1g of adsorbents are given in Table2.

Table 2. Experimental and calculated parameters of pseudo-first and second order kinetic models

Adsorbents		q_e mM/g (exp)	Pseudo-first order model			Pseudo-second order model		
			q_e mM/g	k_1 min^{-1}	R^2	q_e mM/g	k_2 min^{-1}	R^2
0.2 g	HA/Alg	0.4995	0.0989	0.2103	0.8682	0.5048	7.2538	0.9999
	HA/Alg/Gel	0.4993	0.0738	0.2091	0.9394	0.5048	6.8727	0.9999
0.1 g	HA/Alg	0.9999	0.4961	0.3258	0.9988	1.0222	1.6168	0.9999
	HA/Alg/Gel	0.9994	0.3404	0.2075	0.9988	1.0219	1.5193	0.9999

The values of q_e obtained from pseudo-first order equation for both the adsorbent dosages are different from the experimental q_e value. While in the case of pseudo-second order rate equation, the q_e value obtained from the linear plots matched notably with the experimental results. The regression coefficient (R^2) from pseudo-second order rate equation for both the adsorbent dosages are higher when compared to the pseudo-first order equation. These results revealed that the kinetic data of both the adsorbent dosages exhibited best fit to the pseudo-second order equation.

3.4. Adsorption isotherm studies

The values of Langmuir constants for both adsorbent dosages evaluated from the isotherm plots and the parameters such as F - ratio, prob>F, sum of squares errors (SSE) and mean squares errors (MSE) obtained from ANOVA analysis are given in Table 3.

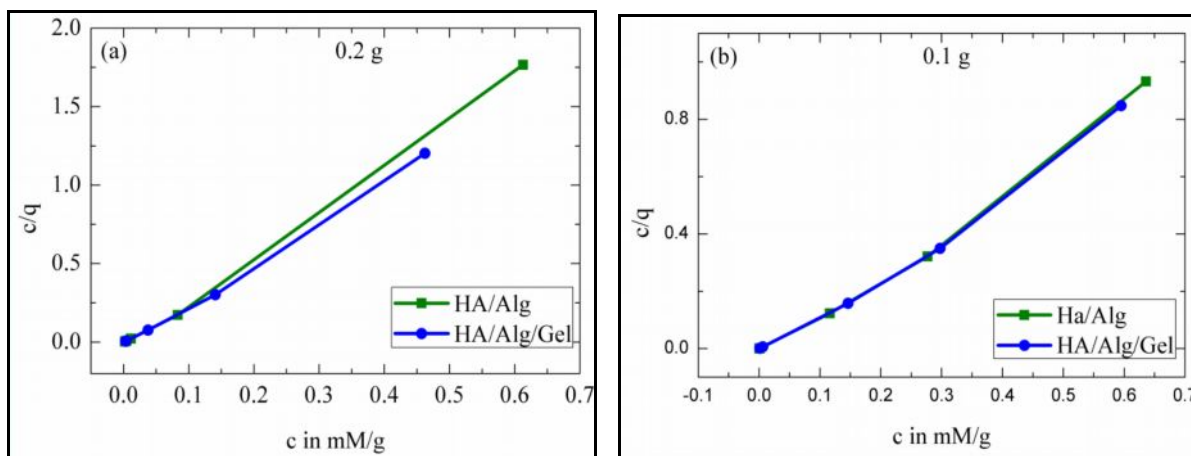
**Fig.5. Langmuir isotherm plots for Pb^{2+} adsorption by the adsorbents**

Table 3. Isotherm and ANOVApараметrs for Langmuir models

Adsorbents/ Parameters	q_{\max}	(-b)	R^2	SSE	MSE	F Value	Prob>F	
0.2 g	HA/Alg	0.3442	149.45	0.9983	0.0030	0.0010	2352	1.93E-5
	HA/Alg/Gel	0.3827	136.45	0.9963	0.0029	0.0010	1076	6.23E-5
0.1 g	HA/Alg	0.6849	58.054	0.9871	0.0059	0.0020	307.9	4.03E-4
	HA/Alg/Gel	0.7080	61.091	0.9872	0.0048	0.0016	309.2	4.01E-4

The regression coefficient obtained for 0.2gofboth adsorbents for Langmuir model are 0.9983, 0.9963 and for Freundlich model are 0.645, 0.597,while for 0.1g are 0.9871, 0.9872 (Langmuir) and 0.4761,0.568 (Freundlich). Hence it is clear that the Langmuir isotherm fits bestto the adsorption of Pb^{2+} and corresponding linearized adsorption isotherm plots for higher and lower dosage of adsorbents are given in Fig.5. Values of q_{\max} (maximum sorption capacity) were found to be high for the adsorbent containing gelatin for both the adsorbent dosages. ANOVA statistical analysis also confirmed that the Langmuir isotherm model fittedvery well to the adsorption for both the dosages than the Freundlich isotherm model.

4. Mechanism of the Pb^{2+} sorption

Mechanism of Pb^{2+} sorption can be predicted from the aqueous pH, Ca and Pb^{2+} ion concentrations and the XRD results. The steadily increasing concentration of Ca^{2+} in the aqueous solution during the sorption (Fig.6. a & b) might be due to the dissolution of HA mineral in the adsorbents as the initial pH of the aqueous medium was 5. The dissolution of HA can be expressed as follows

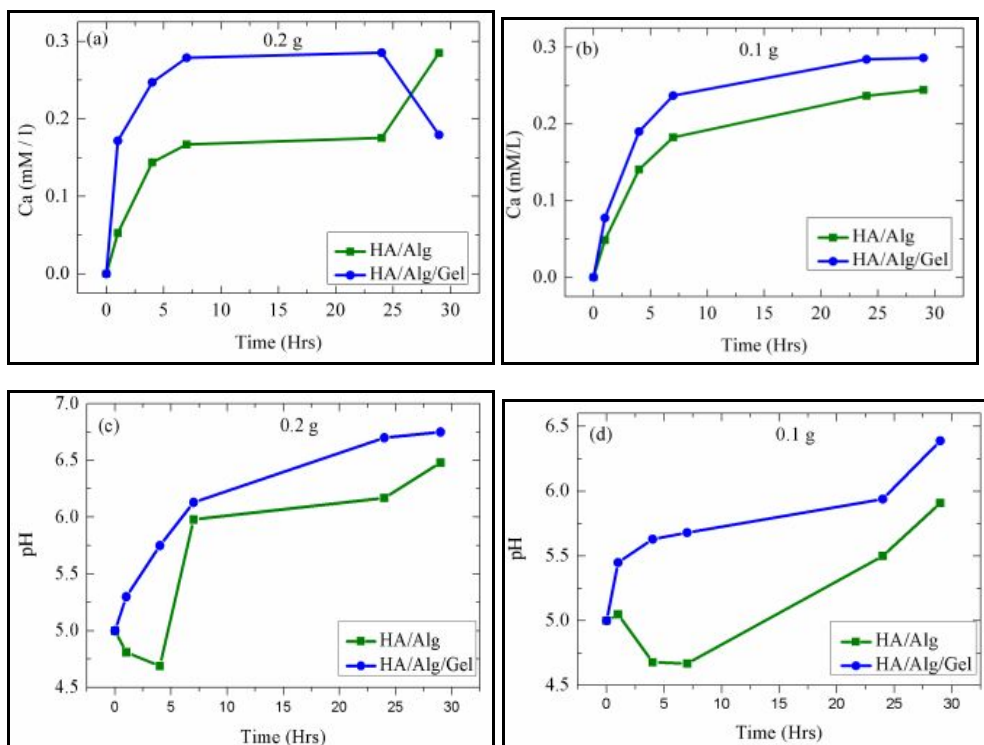
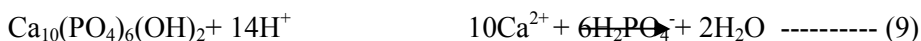
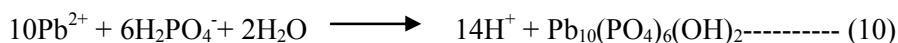
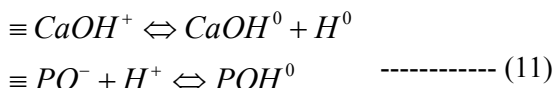


Fig. 7. (a) & (b).Concentration of Ca^{2+} in the adsorption medium; (c) & (d). pH changes of aqueous solution during the experiment

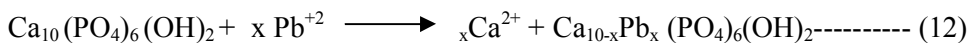
Correspondingly the Pb^{2+} concentration in the solution was steadily decreasing and reached zero at the end of the experiment. This lead ion consumption has resulted in the precipitation of the new phase hydroxypyromorphite as confirmed from the XRD. The precipitation of hydroxypyromorphite¹⁹ can be described by-



During dissolution/precipitation process pH variations should not occur²⁰. But the pH values measured during the experiment decreased slightly for HA/Alg initially (Fig.6. c & d), otherwise pH of the aqueous solution increased significantly. The decrease of pH in HA/Alg could be due to dissociation of carboxyl groups of polymers and exchange of protons between the adsorbent and metal ions in the solutions²¹. The significant increase in pH observed for both the adsorbents may be due to the surface complexation between HA and acidic aqueous solution which can be described^{22,23} as follows



The isomorphic substitution ability of HA can lead to exchange of Ca^{2+} by Pb^{2+} and is evident from the increased lattice parameter values of HA. This ion exchange mechanism between Pb^{2+} ions and Ca^{2+} ions of HA^{24,25} is expressed as



From the above results, we may assume that the lead ion sorption from the aqueous solution by both the adsorbents may be influenced by different mechanisms such as dissolution/precipitation, surface complexation and ion exchange process.

5. Conclusions

In the present study, Pb^{2+} removal ability of wet precipitation synthesized biosorbents HA/Alg and HA/Alg/Gel has been investigated for different dosages. Complete removal was achieved from 7 to 24 hours by both the adsorbents. The sorption kinetics exhibited best fit to the pseudo-second order equation and the equilibrium followed Langmuir isotherm model. The removal capacity was higher for lower dosage studied and the rate of removal was higher for the higher dosage studied. The mechanism of sorption involved was dissolution/precipitation, surface complexation and ion exchange process. These results showed that both the composites evaluated are potential candidates for Pb^{2+} removal and specifically gelatin enhanced the maximum sorption than the alginate alone which is composed with the hydroxyapatite.

Acknowledgments

The author K.S. expresses her sincere thanks to Department of Science and Technology (DST), India (Project Ref. No:SR/WOS-A/PS-15/2011) for financial support.

References

1. C.L. Ake, K. Mayura, H. Huebner, G.R. Bratton and T.D. Phillips, Development of porous clay-based composites for the sorption of lead from water, *J. Toxicol. Environ. Health Part A*, 2001, 63 (6), 459–475.
2. S. Tunali, T. Akar, A.S. Özcan, I. Kiran and A. Özcan, Equilibrium and kinetics of biosorption of lead(II) from aqueous solutions by Cepha-losporium aphidicola, *Sep. Purif. Technol.*, 2006, 47 (3), 105–112.
3. G. Kiley, *Environmental Engineering*, McGraw-Hill, New York, 1997.
4. M. Markowitz, Lead poisoning, *Pediatr. Rev.* 2000, 10, 327–335.
5. J.C. Morris, W.J. Weber Jr., Adsorption of biochemically resistant materials from solution 1, *Public Health Ser-v. Public. 1964*, 999-WP-11.
6. G. Vázquez, M. Calvo, M.S. Freire, J. González-Alvarez, G. Antorrena, Chestnut shell as heavy metal adsorbent: optimization study of lead, copper and zinc cations removal, *J. Hazard. Mater.* 2009, 172, 1402–1414
7. Y. Takeuchi, T. Suzuki, H. Arai, A study of equilibrium and mass transfer in processes for removal of heavy metal ions by hydroxyapatite, *J. Chem. Eng. Jpn.* 1998, 21 (1), 98–100.

8. S. Azabou, T. Mechichi, S. Sayadi, Zinc precipitation by heavy-metal tolerant sulfate-reducing bacteria enriched on phosphogypsum as a sulfate source, Miner. Eng. 2007, 20, 173–178.
9. P. Guillaume, N. Leclerc, F. Lapicque, C. Boulanger, Electroleaching and elec-trodeposition of zinc in a single-cell process for the treatment of solid waste, J.Hazard. Mater. 2008, 152, 85–92
10. D. Mohan, C.U. Pittman Jr., Activated carbons and low cost adsorbents for remediation of tri- and hexavalent chromium from water, J. Hazard. Mater. 2006, 137, 762–811.
11. M. Kazemipour, M. Ansari, S. Tajrobehka, M. Majdzadeh, H.R. Kermani, Removal of lead, cadmium, zinc and copper from industrial wastewater by carbon developed from walnut, hazelnut, almond, pistachio shell and apricot stone, J. Hazard. Mater. 2008, 150, 322–327.
12. C.S. Sundaram, N. Viswanathan, S. Meenakshi, Defluoridation chemistry of synthetic hydroxyapatite at nano scale: equilibrium and kinetic studies, J. Hazard. Mater. 2008, 155, 206–215.
13. V. Ball, J.-M. Planeix, O. Felix, J. Hemmerle, P. Schaaf, M. W. Hosseini, J.C. Voegel, Molecular Tectonics: Abiotic Control of Hydroxyapatite Crystals Morphology, Cryst. Growth Des. 2002, 2, 489–492.
14. C. Stötzel, F.A. Müller, F. Reinert, F. Niederdraenk, J.E. Barralet, U. Gburecka, Ion adsorption behaviour of hydroxyapatite with different crystallinities, Colloids Surf., B. 2009, 74, 91–95.
15. E. Mavropoulos, A.M. Rossi, A.M. Costa, C.A.C. Perez, J.C. Moreira, M. Saldanha, Studies on the mechanisms of lead immobilization by hydroxyapatite, Environ. Sci. Technol. 2002, 36, 1625–1629.
16. S.K. Papageorgiou, F.K. Katsaros, E.P. Kouvelos, J.W. Nolan, H.L. Deit, N.K. Kanellopoulos, Heavy metal sorption by calcium alginate beads from Laminaria digitata, J. Hazard. Mater. 2006, B137, 1765–1772.
17. I. Langmuir, The adsorption of gases on plane surfaces of glass, mica and platinum, J. Am. Chem. Soc. 1918, 40, 1361–1403.
18. K. Sangeetha, A. Thamizhavel, E.K. Girija, Effect of gelatin on the *in situ* formation of Alginate/Hydroxyapatite nanocomposites, Mater Lett. 2013, 91, 27–30.
19. V. Laperche, S.J. Traina, P. Gaddam, T.J. Logan, Chemical and Mineralogical Characterizations of Pb in a Contaminated Soil: Reactions with Synthetic Apatite, Environ. Sci. Technol. 1996, 30, 3321–3326.
20. Q.Y. Ma, S.J. Traina, T.J. Logan, J.A. Ryan, In situ lead immobilization by apatite. Environ. Sci. Technol. 1993, 27, 1803–1810.
21. Xiaohuan Wang, Yian Zheng, Aiqin Wang, Fast removal of copper ions from aqueous solution by chitosan-g-poly(acrylic acid)/attapulgite composites, J. Hazard. Mater. 2009, 168, 970–977.
22. Smiciklas, I., Dimovic, S., Plecas, I., Mitric, M., Removal of Co^{2+} from aqueous solutions by hydroxyapatite. Water Res. 2006, 40, 2267–2274.
23. L. Wu, W. Forsling, P.W. Schindler, Surface complexation of calcium minerals in aqueous solutions. 1. Surface protonation of fluorapatite water interface, J. Colloid Interface Sci. 1991, 147, 178–185.
24. T. Suzuki, K. Ishigaki, M. Miyake, Synthetic hydroxyapatites as inorganic cation exchangers. Part-3. Exchange characteristics of lead ions (Pb^{2+}), J. Chem. Soc. Faraday Trans. 1984, 80, 3157–3165.
25. A. Corami, S. Mignardi, V. Ferrini, Cadmium removal from single- and multi-metal ($\text{Cd}+\text{Pb}+\text{Zn}+\text{Cu}$) solutions by sorption on hydroxyapatite, J. Colloid Interface Sci. 2008, 317, 402–408.
